

Space-time wind speed forecasting for improved power system dispatch

Xinxin Zhu · Marc G. Genton · Yingzhong Gu · Le Xie

Published online: 27 February 2014
© Sociedad de Estadística e Investigación Operativa 2014

Abstract To support large-scale integration of wind power into electric energy systems, state-of-the-art wind speed forecasting methods should be able to provide accurate and adequate information to enable efficient, reliable, and cost-effective scheduling of wind power. Here, we incorporate space-time wind forecasts into electric power system scheduling. First, we propose a modified regime-switching, space-time wind speed forecasting model that allows the forecast regimes to vary with the dominant wind direction and with the seasons, hence avoiding a subjective choice of regimes. Then, results from the wind forecasts are incorporated into a power system economic dispatch model, the cost of which is used as a loss measure of the quality of the forecast

The work of the first two authors was supported in part by NSF Grant DMS-1007504. The work of the last two authors was supported in part by NSF ECCS Grant 1150944. This publication is partly based on work supported by Award No. KUS-C1-016-04 made by King Abdullah University of Science and Technology (KAUST).

This invited paper is discussed in comments available at: doi:[10.1007/s11749-014-0352-z](https://doi.org/10.1007/s11749-014-0352-z), doi:[10.1007/s11749-014-0353-y](https://doi.org/10.1007/s11749-014-0353-y), doi:[10.1007/s11749-014-0354-x](https://doi.org/10.1007/s11749-014-0354-x), doi:[10.1007/s11749-014-0355-9](https://doi.org/10.1007/s11749-014-0355-9).

X. Zhu
Department of Statistics, Texas A&M University, College Station, TX 77843-3143, USA
e-mail: xzhu@stat.tamu.edu

M. G. Genton (✉)
CEMSE Division, King Abdullah University of Science and Technology,
Thuwal 23955-6900, Saudi Arabia
e-mail: marc.genton@kaust.edu.sa

Y. Gu · L. Xie
Department of Electrical and Computer Engineering, Texas A&M University,
College Station, TX 77843-3128, USA
e-mail: gydzmgqy@gmail.com

L. Xie
e-mail: Lxie@ece.tamu.edu

models. This, in turn, leads to cost-effective scheduling of system-wide wind generation. Potential economic benefits arise from the system-wide generation of cost savings and from the ancillary service cost savings. We illustrate the economic benefits using a test system in the northwest region of the United States. Compared with persistence and autoregressive models, our model suggests that cost savings from integration of wind power could be on the scale of tens of millions of dollars annually in regions with high wind penetration, such as Texas and the Pacific northwest.

Keywords Correlation · Cost savings · Power system economic dispatch · Space-time statistical model · Wind energy · Wind speed forecasting

Mathematics Subject Classification (2000) Primary 62J05; Secondary 62P30

1 Introduction

1.1 Wind energy

Renewable energy, particularly wind energy, is rapidly being integrated into electric power systems throughout the world. In Denmark, wind has become one of the largest sources of electricity, supplying 26 % of electricity demand in 2011. In Spain, 15.9 % of electricity consumption was generated by wind in 2011, along with 15.6 and 10.6 % in Portugal and Germany, respectively, according to the European Wind Energy Association (EWEA 2012). The United States (US) Department of Energy (DOE) published a report in 2008 that described a model-based scenario in which wind energy would provide 20 % of US electricity demand by 2030 (DOE 2008). China is pursuing a total capacity of 150 Gigawatts (GW) from wind energy by 2020, 250 GW by 2030 and 450 GW by 2050 (CREIA (2010); see the review by Zhu and Genton (2012) for more information about global wind energy).

Due to the high variability and limited predictability of wind, current power system scheduling methods face challenges in integrating large-scale wind power. The basic objective of power system scheduling is to maintain a supply and demand balance at minimum cost, subject to transmission constraints and plausible contingencies. Prior to the introduction of renewable energy sources, such as wind and solar, uncertainty in power system scheduling primarily came from the demand side (Xie et al. 2011). Now, with the introduction of intermittent wind generation, this uncertainty comes from both supply and demand sides. Highly accurate wind power forecasts are therefore very much needed. Several important pieces of work discuss the major technical challenges in power system operations that integrate large-scale wind energy (Ackermann 2005; Denny and O'Malley 2006; Makarov et al. 2009; Xie et al. 2011).

1.2 Wind speed forecasting

Accurate wind speed prediction is crucial in reducing the uncertainty from the supply side in the power system scheduling. Compared with long-term prediction, short-term forecasting (e.g., hours ahead to minutes ahead) is more accurate and reliable. It is

also essential to effective power system operations. Hours-ahead wind forecasting provides good timing guide for quick-start power to operate and bridge the gap in energy imbalances on time. [Genton and Hering \(2007\)](#) suggested that wind power forecasts by converting wind speed forecasts based on a power curve is one of the common ways for wind power prediction because unpredicted operating conditions (e.g., curtailment) may affect the quality of direct power prediction. Wind farms also usually have different wind turbine models and designs, hence wind speed forecasting is more adaptive to convert to power production forecasts based on their own power curves provided by their manufacturers. Moreover, forecasting based on wind power directly is available only when there is historical wind power data collected from wind farms. Our method is also helpful when the goal is to evaluate the potential wind power production at certain locations before building wind farms there. Therefore, in this paper, we focus on short-term wind speed forecasting with speed/power conversion. Note that more complicated speed/power conversion [e.g., conditional dynamic power curves proposed by [Jeon and Taylor \(2012\)](#)] can further improve the quality of the forecast effectively. The model proposed herein could be adapted to such advanced speed/power conversion technology.

Extensive research has been devoted to wind power forecasting problems. [Giebel et al. \(2011\)](#), [Kariniotakis et al. \(2004\)](#), [Monteiro et al. \(2009\)](#) and [Zhu and Genton \(2012\)](#) reviewed approaches to wind power forecasting, including physical methods, statistical models and combined physical-statistical systems. In short-term wind speed forecasting, statistical models have been found to be quite competitive compared with other approaches. Moreover, statistical models that incorporate spatial information are more accurate than the conventional time series models [see [Zhu and Genton \(2012\)](#) for a review]. [Gneiting et al. \(2006\)](#) proposed a regime-switching space-time diurnal (RSTD) model to forecast 2-h-ahead wind speed at Vansycle, Oregon. Their model outperformed persistence forecasts and autoregressive forecasts by 29 and 13 %, respectively, in terms of the root mean squared error (RMSE) in July 2003, for instance. However, the RSTD model relies on local geographic features. To remove these constraints, [Hering and Genton \(2010\)](#) generalized the RSTD model by treating wind direction as a circular variable and including it in their model. They coined it a trigonometric direction diurnal (TDD) model. The TDD model obtained similar or better forecasting results than did the RSTD model without requiring prior geographic information. [Tastu et al. \(2011\)](#) analyzed and modeled short-term wind power forecast errors using spatio-temporal methods, such as regime-switching models based on wind direction and conditional parametric models with regime-switching, substantially reducing variance in the forecast errors. [Pinson and Madsen \(2012\)](#) applied adaptive Markov-switching autoregressive models to offshore wind power forecasting problems in which the regime sequence is not directly observable, but follows a first-order Markov chain. Here, we propose a new modification of the RSTD model to allay its limitations.

Model evaluation is also an important step in making a final decision on which model should be implemented. Usually, a loss function is predefined and the model that can generate forecasts with the smallest loss is considered to be the most advanced; see [Gneiting \(2011\)](#). Squared and absolute errors are two commonly used loss functions. However, for wind forecasting problems, more realistic loss functions are needed since

penalization on underestimates and forecasts of small true values are desired; see [Zhu and Genton \(2012\)](#) for a more detailed discussion. [Hering and Genton \(2010\)](#) proposed the power curve error as a loss function, which links prediction of wind speed to wind power by a power curve and evaluates the loss based on the wind power with penalty on underestimates. [Zhu and Genton \(2012\)](#) introduced the mean absolute percentage error and the mean symmetric absolute percentage error as loss functions to penalize both underestimates and forecasts of small true values. In this paper, we propose a new idea for model evaluation based on the power system operating costs. Since the ultimate goal is to reduce the cost of the whole power system, it is natural to look for the forecasts generated from a model that produces the most cost savings.

In summary, the main contributions of this paper are the following:

1. A modified RSTD model for short-term wind speed forecasting is proposed. It generalizes the RSTD model by allowing the forecast regimes to vary with the dominant wind direction in each season instead of fixing the forecast regimes based on prior geographic information. In the original application of the RSTD model, it was straightforward to define west and east forecast regimes due to prevailing westerly winds in the target area. However, for other settings where the winds follow more complicated patterns, the number and position of the forecast regimes are difficult to determine. In the modified model, the best position of the forecast regimes is detected by rotating the dividing angles of the regimes until the minimum mean absolute error (MAE) for each season is reached. We call this new model RRSTD for rotating RSTD.
2. To evaluate the model, we formulate an economic dispatch model for power systems that incorporates space-time wind forecast information. Numerical simulations are conducted in a representative test system derived in the northwest region of the US, and the results demonstrate the economic benefits from improved wind forecasts.

This paper is organized as follows. In Sect. 2, we first introduce our modified space-time statistical model for short-term wind speed forecasting, the RRSTD model, and then we describe persistence and autoregressive models as references for later comparisons. In Sect. 3, the newly proposed RRSTD model is then applied to a spatio-temporal wind data set from the northwest region of the US. Its prediction MAE values for each month are compared with reference models. In Sect. 4, we propose an economic dispatch model that incorporates available short-term, space-time wind power forecasts. An illustrative power system economic dispatch example for the Pacific northwest is presented, which quantifies the potential savings in both generation costs and ancillary services in the proposed dispatch model. Concluding remarks are provided in Sect. 5.

2 The rotating RSTD model

In this section, we describe the RRSTD model in detail while the RSTD model is included as a special case. As a modification, the RRSTD model keeps the basic characteristics of the RSTD, but overcomes some of its limitations to have more general applicability. Two reference models are also briefly introduced.

2.1 RRSTD model description

Let $y_{s,t}$ and $\theta_{s,t}$ respectively be wind speed and direction at site s and time t , where $s = 1, \dots, S, t = 1, \dots, T$, and $\theta_{s,t} \in [0^\circ, 360^\circ)$ with $0^\circ, 90^\circ, 180^\circ, 270^\circ$ indicating southerly, easterly, northerly and westerly winds, respectively. The objective is to predict $y_{s,t+k}$, the k -step-ahead wind speed at site s , where $k = 1, 2, \dots$. When $k = 1$, for example, depending on the resolution of the wind data, it is a 1-h-ahead forecasting for hourly wind data, and 10-min-ahead forecasting for 10-min wind data. To simplify, we present the RRSTD model in the setting of forecasting wind speed k -step-ahead at a site s_1 , say.

Rather than only providing a deterministic point forecast of $y_{s,t+k}$, a predictive distribution is considered to capture the probabilistic information in wind speed. Since wind speed is non-negative and has large values with low probabilities (right-skew distributed), it is assumed that $Y_{s_1,t+k}$ follows a truncated normal distribution with center and scale parameters $\mu_{s_1,t+k}$ and $\sigma_{s_1,t+k}$: $Y_{s_1,t+k} \sim N^+(\mu_{s_1,t+k}, \sigma_{s_1,t+k})$. To predict $y_{s_1,t+k}$ precisely, the key lies in appropriately modeling $\mu_{s_1,t+k}$ and $\sigma_{s_1,t+k}$. This distribution is used quite commonly in probabilistic wind forecasting models; see [Gneiting et al. \(2006\)](#) and [Zhu and Genton \(2012\)](#) for more discussion.

Generally, seasonal and diurnal patterns are observed in winds. As in the RSTD model, we fit the diurnal pattern with two pairs of harmonics as

$$D_{s_1,h} = d_0 + d_1 \sin\left(\frac{2\pi h}{24}\right) + d_2 \cos\left(\frac{2\pi h}{24}\right) + d_3 \sin\left(\frac{4\pi h}{24}\right) + d_4 \cos\left(\frac{4\pi h}{24}\right), \tag{1}$$

where h indicates the hour of a day, $h = 1, 2, \dots, 24$, and the coefficients are estimated by the least squares method. Then, the center parameter is modeled as $\mu_{s_1,t+k} = D_{s_1,t+k} + \mu_{s_1,t+k}^r$, where $\mu_{s_1,t+k}^r$ is the residual wind speed after removing the diurnal pattern.

The residual, $\mu_{s_1,t+k}^r$, is modeled by a linear combination of historical wind speed residuals, up to p -step lags, of itself as well as its neighbors (to take the spatio-temporal correlations in wind into account), allowing the coefficients to vary with the dominant wind direction and season by defining the variable forecast regimes as

$$\mu_{s_1,t+k}^r = \alpha_0 + \sum_{s=1}^S \sum_{j=0}^p \alpha_{s,j} \left(\theta_{s^*,t}, \theta_{m(t+k)}^* \right) \mu_{s,t-j}^r, \tag{2}$$

where α_0 and $\alpha_{s,j}(\cdot, \cdot), s = 1, \dots, S$ and $j = 0, \dots, p$ are coefficients, and $\theta_{m(t+k)}^* \in [0^\circ, 360^\circ)$ defines the forecast regimes based on the prevailing wind direction in the season (here month), $m(t+k)$, to which time $t+k$ belongs. Here, $\theta_{s^*,t}$ is the current wind direction at site s^* used to indicate the direction of the nearby future wind. The site $s^* \in \{1, \dots, S\}$ is located upstream of the wind and indicates the wind source.

The meaning of the above model is that, for a certain season, if the future wind direction at the target site, which is estimated by $\theta_{s^*,t}$, falls into a predefined forecast

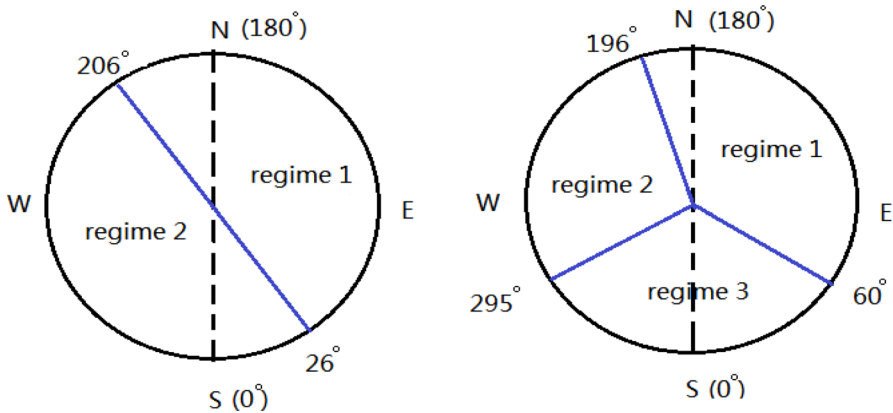


Fig. 1 Regime dividing plots for $\theta_{m(t+k)}^* = \{26^\circ, 206^\circ\}_{Aug}$ (left) and $\theta_{m(t+k)}^* = \{60^\circ, 196^\circ, 295^\circ\}_{Aug}$ (right). The dashed line connects the south (0°) and the north (180°), with the westerly wind to the left and the easterly wind to the right. Separate models of $\mu_{s,t+k}^r$ are built for each regime

regime, a particular space-time linear model will be applied to estimate $\mu_{s_1,t+k}^r$, and the forecast regimes will be based on the dominant wind in that season. For example, if $\theta_{m(t+k)}^* = \{26^\circ, 206^\circ\}_{Aug}$ and $s^* = s_2$, then, in August, the RRSTD model fits two separate models for the center parameters $\mu_{s_1,t+k}^r$: model 1, when the current wind direction at site s_2 is between 26° and 206° , or $\theta_{s_2,t} \in [26^\circ, 206^\circ]$; model 2, when $\theta_{s_2,t} \in [206^\circ, 360^\circ] \cup [0^\circ, 26^\circ]$; see Fig. 1 (left panel). The dimension of $\theta_{m(t+k)}^*$ indicates the number of regimes that are defined. For $\theta_{m(t+k)}^* = \{60^\circ, 196^\circ, 295^\circ\}_{Aug}$ and $s^* = s_2$, three separate models are built for the three forecast regimes divided by these angles; see Fig. 1 (right panel).

The scale parameter $\sigma_{s_1,t+k}$ is modeled as

$$\sigma_{s_1,t+k} = b_0 + b_1 v_{s_1,t}, \quad (3)$$

where $b_0, b_1 > 0$ and $v_{s_1,t}$ is the volatility value: $v_{s_1,t} = \{\frac{1}{2S} \sum_{s=1}^S \sum_{i=0}^1 (\mu_{s,t-i}^r - \mu_{s,t-i-1}^r)^2\}^{1/2}$; see Gneiting et al. (2006) for more information.

A key point of the RRSTD model is how to decide the number and the position of the regimes. For locations that have significant prevailing wind, this can be determined practically (see Sect. 3.2). The RSTD model is a special case of the RRSTD model with $\theta^* = \{0^\circ, 180^\circ\}$, motivated by the westerly prevailing wind in the northwest region of the US. For other situations, we propose that $\theta_{m(t+k)}^*$ be chosen by minimizing the prediction MAE for each season/month after determining the number of regimes. The predictors in (2) are selected by the Bayesian Information Criterion as in Hering and Genton (2010). The coefficients in (2) along with b_0, b_1 in (3) are estimated by means of the continuous ranked probability score method (see Gneiting and Raftery (2007) for more details).

With the estimated predictive distribution, $N^+(\mu_{s_1,t+k}, \sigma_{s_1,t+k})$, we take the median of the truncated normal distribution as the wind speed forecast k -step-ahead at s_1 , defined as

$$z_{0.5}^+ = \mu_{s_1,t+k} + \sigma_{s_1,t+k} \cdot \Phi^{-1} \left\{ 1/2 + \Phi \left(\frac{-\mu_{s_1,t+k}}{\sigma_{s_1,t+k}} \right) / 2 \right\},$$

where $\Phi(\cdot)$ is the cumulative distribution function of a standard normal distribution. The median of the predictive distribution is used as the forecast, because we are using MAE as one of the options to evaluate the performance of the models. As a commonly used metric in model evaluation, MAE fits the context of power system economic analysis appropriately. In the existing industrial practice, what matters to the power system operation is the wind generation deviation. A large deviation can cause extra costs and efforts due to re-dispatch, spinning reserve, and even loss of load. Therefore, we select MAE for performance evaluation of the models although other metrics could be used as well (e.g., RMSE).

2.2 Reference models

To evaluate the performance of the RRSTD model, we compare its forecasts to other models, including the persistence (PSS) and autoregressive (AR) models. The main ideas of the two reference models are introduced briefly:

- PSS assumes that the future wind speed is the same as the current one, or $\hat{y}_{s_1,t+k} = y_{s_1,t}$.
- An AR(p) model estimates $\mu_{s_1,t+k}^r$ in (2) as a linear combination of the previous p wind speed residuals from the same location only, or $\mu_{s_1,t+k}^r = \alpha_0 + \sum_{j=0}^p \alpha_j \mu_{s_1,t-j}^r$. For the scale parameter, a GARCH(1,1) model is used instead of (3); see [Gneiting et al. \(2006\)](#).

Due to the high variations in wind, PSS works better for very short-term forecasting, such as 10-min-ahead predictions. The AR(p) model can capture the temporal correlation in wind patterns and usually outperforms PSS in short-term wind speed forecasting problems.

3 Numerical experiments

3.1 Wind data

The data considered here are 10-min wind speed (m/s) and direction (degrees) records from three meteorological towers located at Vansycle (Oregon), Kennewick (Washington), and Goodnoe Hills (Washington) in the Columbia River Basin, which is in northwest US. Missing data were imputed by linear interpolation. Detailed information about the data and the three sites can be found in [Gneiting et al. \(2006\)](#).

The training and testing data sets were divided as follows:

- Training set: data from 1 August to 30 November 2002. With the training data, for each month, the regime dividing angles, θ^* , and the wind source indicator, s^* , in (2) are learned by minimizing the prediction MAE values. Then, in each forecasting regime, linear models for the center parameter are obtained.

- Testing set: data from 25 February to 30 November 2003. The trained models are evaluated during this period. The parameters in the models are estimated from data that are up to 45 days earlier, as suggested by [Gneiting et al. \(2006\)](#).

3.2 Exploratory data analysis

An exploratory data analysis was conducted on the relationship between wind speed and wind direction with the aim to determine the number of forecast regimes and how to divide the regimes in the RRSTD model. The wind roses in Fig. 2 give a view of how wind speed and wind direction are distributed each month from August to November 2002 at Vansycle (left column), Kennewick (middle column), and Goodnoe Hills (right column). In a wind rose, each petal indicates the frequency of winds blowing from a particular direction, and the color bands in each petal show the range of wind speeds.

As we can see from the wind roses, the wind patterns in this area are quite significant. High frequencies and wide speed ranges are found in the northwest, north and west direction at Vansycle, Kennewick and Goodnoe Hills, respectively, over the four months, followed by winds from the opposite directions. These are consistent with the geographic features in this area, namely, that these three locations are along the south, southwest, and north bank of the Columbia River, which runs from east to west along the boundary between Washington and Oregon, with high terrain in both the north and south restricting the air flow.

Based on these wind patterns, using two forecasting regimes is reasonable. In our experiment, we used two equally divided regimes resulting in a two-regime RRSTD model. More complex RRSTD models with two regimes of different sizes or with multiple (more than two) forecasting regimes could be considered as well. Our exploration of those alternate models revealed insignificant improvements for this particular data set.

3.3 Training data results

The two-regime RRSTD model for each month was trained based on the training data set at all three locations for 1-h-ahead wind speed forecasting. The gains from using the RRSTD model instead of the RSTD are shown in the MAE values in each month in Fig. 3.

Let $y_{V,t}$, $y_{K,t}$, $y_{G,t}$, $\theta_{V,t}$, $\theta_{K,t}$, and $\theta_{G,t}$ denote the wind speed and direction at Vansycle, Kennewick and Goodnoe Hills. The goal here is to predict $y_{V,t+6}$, $y_{K,t+6}$ and $y_{G,t+6}$ (1-h-ahead is equal to 6-steps-ahead in 10-min data). The objective of the training procedure is to find the two-regime dividing angle, $\theta_{m(t+6)}^*$, the wind source indicator, s^* , and the predictors for each forecast regime in (2) with minimum prediction MAE value. To do this, a dense number of possible two-regime forecasting designs are tested. Specifically, for a possible dividing angle, $\theta \in \{1^\circ, 2^\circ, \dots, 180^\circ\}$, a wind source indicator, s^* , is detected with the method used in [Gneiting et al. \(2006\)](#); then, a separate forecasting model is built for each forecasting regime, resulting in prediction MAE values as displayed in Fig. 3 at Vansycle. The blue dashed line in Fig. 3 gives the best two-regime dividing angle, θ^* , with the smallest MAE value.

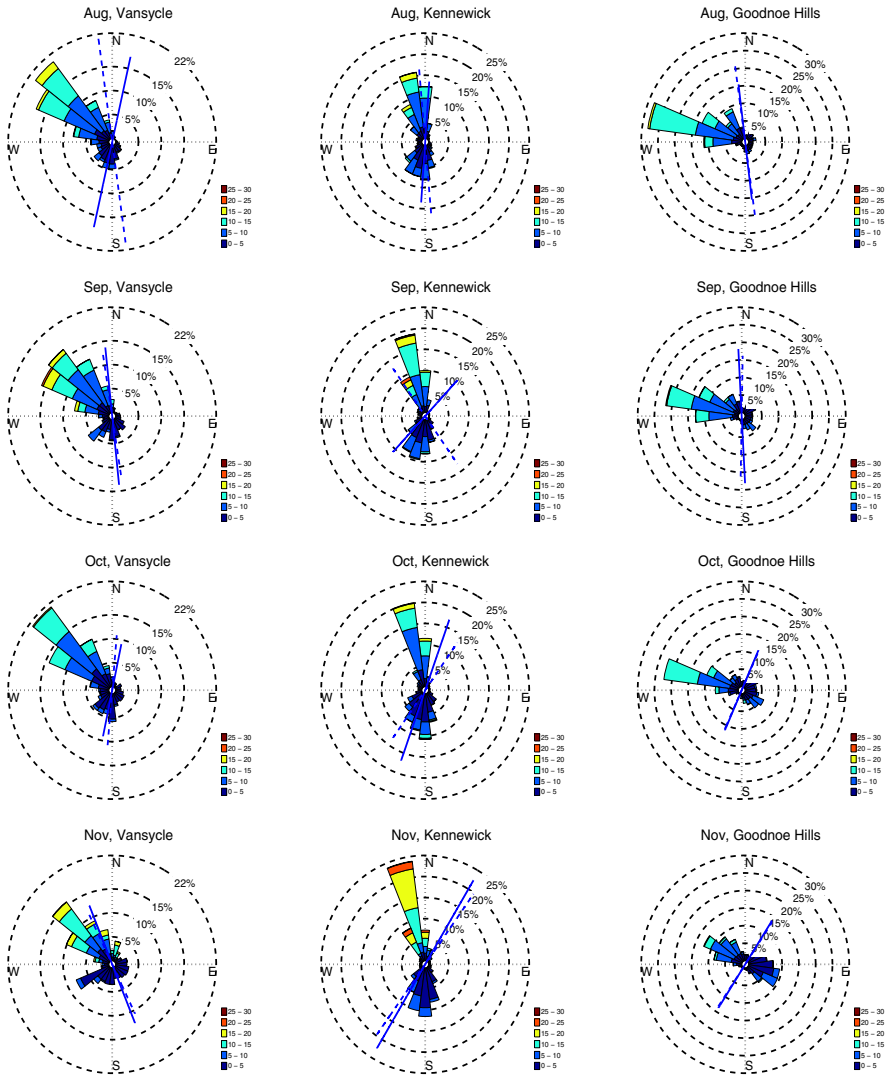


Fig. 2 Wind roses of data from August to November 2002 at Vansycle (left column), Kennewick (middle column) and Goodnoe Hills (right column). The vertical dotted lines give the west-east forecast regimes of the RRSTD (i.e., RSTD) model, while the blue dashed lines and solid lines give the two forecast regimes of the two-regime RRSTD models with the minimum prediction MAE values for each month for 1-h-ahead and 2-h-ahead forecasting, respectively

The RSTD model is a special case of the RRSTD model when the regime dividing angle, θ , is equal to 0° or 180° . As shown in Fig. 3, the minimum MAE value occurs neither at $\theta = 0^\circ$, nor at $\theta = 180^\circ$, while the RRSTD model achieves the smallest MAE value at $\theta = 8^\circ, 9^\circ, 175^\circ$ and 29° for August, September, October, and November, respectively, at Vansycle. The blue solid lines in Fig. 2 give the best two regimes of the two-regime RRSTD models based on the MAE values for each month for 2-h-ahead forecasting. We see that although the westerly wind dominates this area, a simple west-

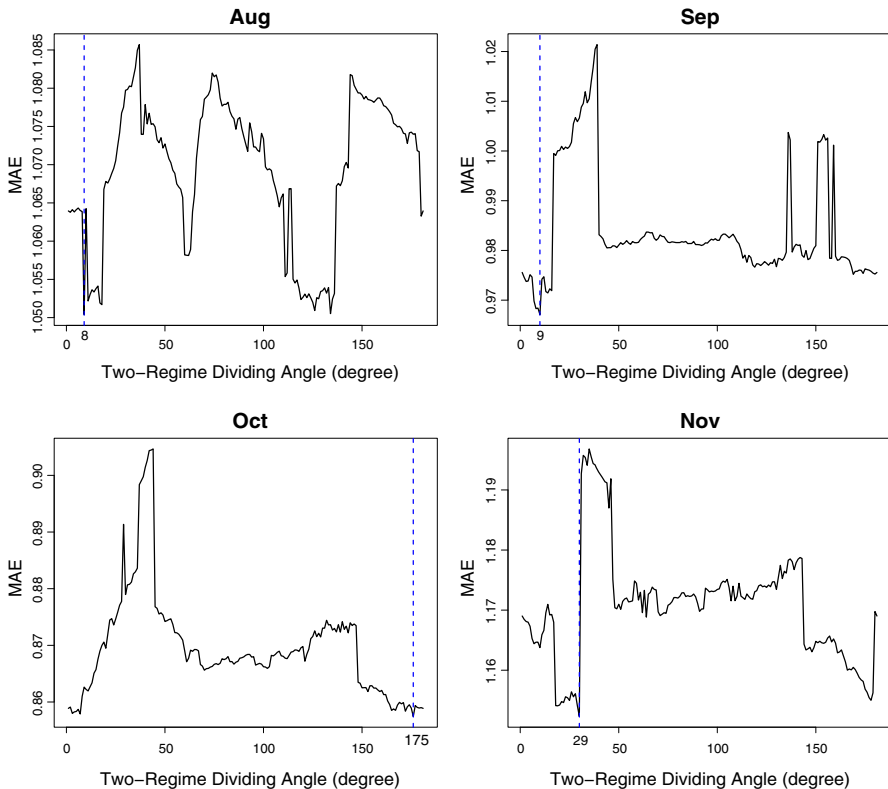


Fig. 3 Plots of 1-h-ahead prediction MAE results based on the two-regime RRSTD model with the dividing angle, θ , from 0° to 180° for each month at Vansycle in 2002. The *blue dashed line* indicates the position of the best two-regime dividing angle, or θ^* , that has the smallest MAE value

east forecast regime is not the best and adjustment is needed for different seasons to achieve more accurate forecasts. The RRSTD model is able to adjust the forecasting regimes to the wind roses shown in Fig. 2 based on wind direction and season. Similar training results are found for the other two locations.

3.4 Testing data results

The trained two-regime RRSTD model for each month is applied to forecast 1-h-ahead wind speed in the same month in the testing data set at all three locations, and the prediction MAE values are compared with the two reference models (see Table 1). Due to data limitations, the model for August is implemented to forecast wind speed in May, June and July in the testing data, and a 45-day training period is used to estimate the coefficients in (2). The results show that the RRSTD model outperforms the PSS and AR models as expected. The latter is fitted with a maximum order of nine based on the Akaike Information Criterion (AIC).

Overall, the RRSTD model outperforms PSS, reducing the MAE value by 8.1 %, and by 6.6 % compared with the AR model at Vansycle. We also conducted 2-h-ahead

Table 1 MAE values of forecasts in the 2003 testing data set based on the two-regime RRSTD models for 1-h-ahead forecasting at Vansycle, Kennewick and Goodnoe Hills, compared with the PSS and AR models

Testing		MAE							
Sites	Models	May	Jun	Jul	Aug	Sep	Oct	Nov	Overall
Vansycle	PSS	1.27	1.18	1.27	1.23	1.19	1.31	1.23	1.24
	AR	1.25	1.16	1.19	1.21	1.19	1.31	1.23	1.22
	RRSTD	1.16	1.06	1.10	1.12	1.11	1.25	1.17	1.14
Kennewick	PSS	1.43	1.28	1.39	1.34	1.26	1.44	1.35	1.36
	AR	1.46	1.27	1.36	1.33	1.25	1.44	1.33	1.35
	RRSTD	1.40	1.23	1.33	1.30	1.23	1.44	1.35	1.33
Goodnoe Hills	PSS	1.17	1.14	1.12	1.15	1.18	1.33	1.28	1.20
	AR	1.13	1.09	1.03	1.12	1.17	1.30	1.26	1.16
	RRSTD	1.11	1.08	1.02	1.09	1.12	1.29	1.22	1.13

The smallest MAE values are in bold

forecasting experiments and experiments with the RSTD and TDD models, and similar results overall were obtained. Wind roses from May to November 2003 at Vansycle are depicted in Fig. 4. In fact, with only 4 months of training data, the forecasting ability of the RRSTD model is challenged by the assumption that monthly patterns remain similar in the training and testing data, while at least several years of wind data would be needed to model monthly patterns. We believe that the performance of the RRSTD model would be better if more data were available.

4 Integrating wind power into a power system

In this section, we incorporate space-time wind forecasts into electric power system scheduling. We compare the system-wide generation cost savings, as well as the ancillary service cost savings, using the RRSTD, AR, PSS forecasting models. First, a test system based on the Bonneville Power Administration (BPA) system, which covers the area where the wind data were collected, is introduced and studied for power system operation with space-time wind forecasts. Second, we formulate the power system dispatch problem that incorporates advanced spatio-temporal correlated wind forecasts. Finally, a numerical experiment is conducted and analyzed, and the performances of the different forecasting models are compared.

4.1 Power system specification in the BPA region

A power system economic dispatch model is used by system operators in scheduling power generation. This model determines the power generators' outputs to maintain a balance between supply and demand, as well as to minimize total system operating costs while satisfying security constraints. In this subsection, a detailed power system dispatch procedure is introduced based on the BPA system, which covers the areas of Vansycle, Kennewick and Goodnoe Hills.

Established in 1937, BPA is a non-profit agency located in the Pacific northwest. About one-third of the electric power used in the northwest comes from BPA,

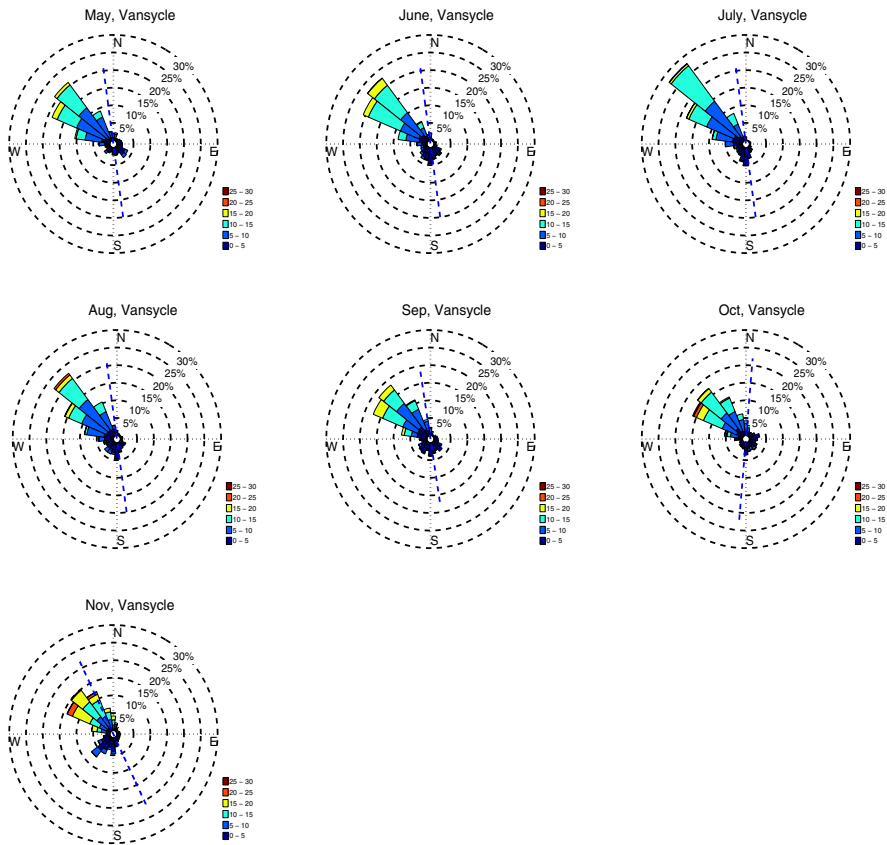


Fig. 4 Wind roses from May to November 2003 at Vansycle. The vertical dotted lines give the west-east forecast regimes of the RRSTD (i.e., RSTD) model, while the blue dashed lines give the two forecast regimes of the two-regime RRSTD models with minimum prediction MAE values for each month for 1-h-ahead forecasting

which operates and maintains about 75 % of the high-voltage transmission network (15,212 circuit miles) in its service territory (BPA 2010), which includes Idaho, Oregon, Washington, western Montana and small parts of eastern Montana, California, Nevada, Utah and Wyoming (Fig. 5).

The major missions of BPA in operating electric energy are to: (1) act as an adequate, efficient, economical and reliable power supply; and to (2) maintain a transmission system capable of integrating different power resources, providing electricity to its customers through inter-regional interconnections and maintaining electrical reliability and stability.

To balance demands for power, the output of every generator in the system has to be scheduled over different time frameworks (i.e., day-ahead, hour-ahead, and 5- to 10-min-ahead). The BPA scheduling procedure (Makarov et al. 2008) is shown in Fig. 6. In the power generation scheduling process, the system operator at BPA schedules generators to meet the expected demand over several time scales. All the scheduled power generation must be within the output capacity, as well as within the ramping

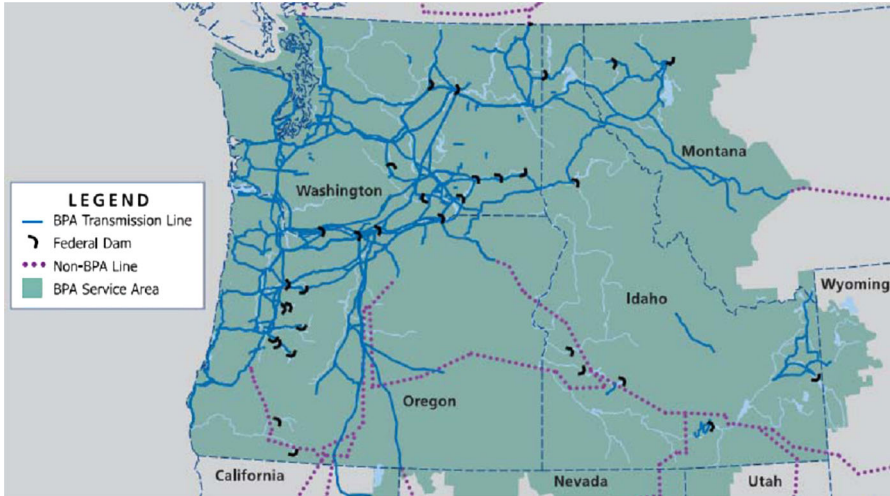


Fig. 5 BPA’s transmission system including Idaho, Oregon, Washington, Montana and Wyoming (BPA 2010)

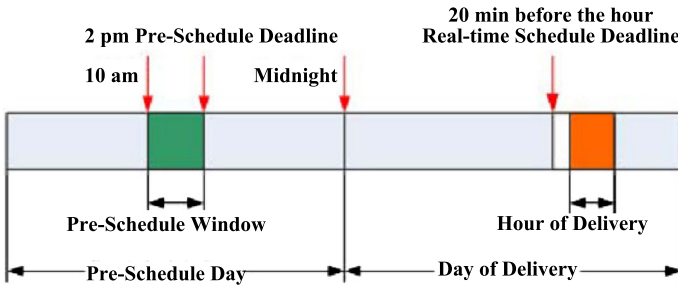


Fig. 6 BPA’s scheduling procedure (Makarov et al. 2008)

capacity, which refers to the maximum change in power generation output between two consecutive time intervals. For example, a natural gas generator’s ramping capacity can be 15 % of its maximum output in 10 min.

Given that it takes several hours to start up or shut down many large generators (e.g., nuclear, coal), a day-ahead schedule (or pre-schedule) process is required to plan the generators’ operations over the next 24 h. Based on day-ahead forecasts, the pre-schedule is completed before 2:00 pm the day before the day-of-delivery (or the day on which the real-time operation takes place). However, the day-ahead load forecast and day-ahead wind forecast have relatively low accuracies, therefore a real-time schedule that is 1-h ahead in BPA is required to discern a mismatch between the near-term forecast and the day-ahead forecast. The real-time schedule is established on the hour-ahead forecast, which has to be completed 20 min before the hour-of-delivery (the hour when the real-time operation takes place).

Within each hour, the available wind generation, as well as the electricity demand, still varies from second to second. Such an imbalance between total supply and total demand will cause degradation of the frequency of the electricity, which has very stringent requirements for the safety of many appliances. In order to maintain the

system's electrical frequency at 60 Hz, automatic feedback control loops are installed at many generators' speed governors, which is referred to as the automatic generation control mechanism and is very similar in principle to the cruise control in automobiles.

4.2 Power system dispatch with space-time wind forecasts

Motivated by the development of wind energy, there is now a large body of literature on understanding the impact of wind power on electricity grid operations. [Watson et al. \(1994\)](#) first introduced the numerical weather prediction (NWP) model for power system scheduling and evaluated its benefits (on-line reserve planning) to the England and Wales National Grid. Later, autoregressive moving average (ARMA) models were used for wind forecasting and incorporated into power dispatch models ([Tuohy et al. 2009](#); [Soder 2004](#)). Developed from conventional criteria, probabilistic optimal dispatch methods were proposed to quantify the spinning/non-spinning reserve requirements for integrating wind ([Bouffard and Galiana 2008](#); [Doherty and O'Malley 2005](#)). The spinning reserve is the extra generating capacity from units that are already turned on and are capable of increasing the power output when needed. The non-spinning reserve is the extra generating capacity that is not currently connected to the system, but can be brought online after a short delay. In recent years, many efforts have focused on enhanced day-ahead power system operation using NWP models ([Constantinescu et al. 2011](#); [Pappala et al. 2009](#)). To handle potential risks posed by wind generation, advanced dispatch methods such as robust optimization ([Zhao and Zeng 2010](#)) and stochastic optimization ([Constantinescu et al. 2011](#); [Wang et al. 2008](#); [Wu et al. 2007](#); [Meibom et al. 2011](#); [Papavasiliou et al. 2011](#)) based unit commitment (UC)/economic dispatch (ED) models were proposed and studied. Unit commitment makes the start-up/shut-down decisions of generators toward the least-cost dispatch of available generation resources to meet the electrical load. Economic dispatch provides the generation output dispatch decisions which specify the output level of each generator toward a minimized total operating cost to balance the load.

Although there have been many different proposals on what should be an optimal dispatch method in future power systems, actual practice during real-time operations is still a *single-stage* security-constrained economic dispatch (SCED). Our aim is to assess the economic value brought by the RRSTD model using a well-accepted industry model in real-time power system operations. In other words, the power system dispatch model is assumed to be a single-stage SCED. Consequently, we neglect the time step index for decision variables and parameters in the formulation. The mathematical formulation of the single-stage SCED is described as follows with the notation listed in Table 2:

$$\min_{P_{G_i}, P_{W_i}, P_{R_i}} : \sum_{i \in G} C_{G_i}(P_{G_i}) + \sum_{i \in W} C_{W_i}(P_{W_i}) + \sum_{i \in G} C_{R_i}(P_{R_i}), \quad (4)$$

subject to:

$$\sum_{i \in G} P_{G_i} + \sum_{i \in W} P_{W_i} = \sum_{i \in D} P_{D_i}, \quad (5)$$

Table 2 Notation for the power system dispatch model

G	Set of conventional power plants
D	Set of inelastic loads
W	Set of wind farms
C_{G_i}	Generation cost function of power plant i
C_{W_i}	Generation cost function of wind farm i
C_{R_i}	Reserve cost function of power plant i
P_{G_i}	Scheduled generation of power plant i
P_{W_i}	Scheduled generation of wind farm i
P_{D_i}	Forecasted load level of bus i
P_{R_i}	Scheduled reserve capacity of power plant i
\mathbf{F}	Vector of branch flows
\mathbf{F}^{\max}	Vector of capacity limits of transmission lines
ΔT	Energy Market scheduling interval
P_i^R	Ramping constraints of power plants i
$P_{G_i}^{\min}$	Lower operating limit of power plant i
$P_{G_i}^{\max}$	Higher operating limit of power plant i
$P_{W_i}^{\min}$	Lower operating limit of wind farm i
$P_{W_i}^{\max}$	Higher operating limit of wind farm i
\hat{P}_{W_i}	Forecasted wind availability for wind farm i

$$\sum_{i \in G} P_{R_i} \geq R_D + R_W, \tag{6}$$

$$|\mathbf{F}| \leq \mathbf{F}^{\max}, \tag{7}$$

$$|P_{G_i} - P_{G_i}^0| \leq P_i^R \Delta T, i \in G \cup W, \tag{8}$$

$$P_{G_i}^{\min} \leq P_{G_i} \leq P_{G_i}^{\max}, \tag{9}$$

$$0 \leq P_{R_i} \leq P_{G_i}^{\max}, \tag{10}$$

$$P_{G_i}^{\min} \leq P_{G_i} + P_{R_i} \leq P_{G_i}^{\max}, \tag{11}$$

$$P_{W_i}^{\min} \leq P_{W_i} \leq P_{W_i}^{\max}, \tag{12}$$

$$P_{W_i} \leq \hat{P}_{W_i}. \tag{13}$$

In the proposed formulation, the objective function (4) is to minimize the power system’s operating costs, which include costs of power generation and costs of providing reserve and regulation services. The decision variables include: the dispatched generation output for each generator, P_{G_i} ; the dispatched generation output for each wind farm, P_{W_i} ; the dispatched generation output for regulation and reserve capacity, P_{R_i} . Constraints on this problem include system and individual unit operating constraints posed by security and reliability. The energy balance Eq. (5) requires that the total power generation always satisfies the total demand in the steady state. The system’s reserve and regulation requirements (6) are determined by the reliability requirement component of the load, R_D , and the reliability requirement component of wind generation, R_W . The load component is a linear function of actual

Table 3 BPA's integrated resources (BPA 2010)

Type	Sustained capacity (MW)	Percentage
Hydro	27,142	59.5
Coal	5,866	12.9
Combustion turbines	5,526	12.1
Co-generation	2,938	6.4
Nuclear	1,150	2.5
Imports	2,094	4.6
Non-utility	630	1.4
Other resources	258	0.6

system-wide load levels for each interval as practiced by major independent system operators (ERCOT 2010). The reserve requirement related to wind generation, R_W , is a linear function of the MAE of the wind generation forecast error. The transmission line capacity limitations (7) contribute to network transmission congestion. The ramping constraints of generators are described by (8). The upper bounds and lower bounds of conventional generators' outputs are provided by (9). The available reserve and regulation capacity constraints are given by (10). The wind component is given by the deviation between the actual wind generation production potential and the wind generation forecast. This approach to quantifying system reserve requirements approximates the empirically based approach to quantifying reserve requirements and serves as a lower bound for the reliability requirement due to wind forecast uncertainty. The capacity constraints of each generator for providing both energy and reserve services are in (11). The upper and lower bounds of wind farms' power output are described by (12). The wind forecast for each wind farm is provided by (13). This is determined by a space-time forecast model, for instance the RRSTD.

4.3 A realistic illustrative example

In this subsection, numerical simulations are performed in a test BPA system. We adopt the current real-time operational practice in the power industry, which is a single-stage, security-constrained economic dispatch model. The wind speed forecasts in Sect. 3 are converted into wind power forecasts with a 2.5 MW Nordex power curve for each wind turbine and scaled up to wind farms based on the BPA system setup. According to the economic dispatch results, different wind forecasting models are compared in terms of potential savings in both generation cost and ancillary services.

Vansycle, Kennewick and Goodnoe Hills are located in the Columbia River Basin. The electric power grid of this area is operated by BPA. Our simulation system is revised from the IEEE Reliability Test System (RTS-24) (Grigg et al. 1999). The generators are categorized as different technology-based power resources, such as hydro, coal, nuclear, natural gas and wind power. The generator capacity portfolio (installed capacity percentage of different technologies) is configured according to the generation portfolio of the practical BPA system (BPA 2010) (see Table 3). The network typology of the simulation system is presented in Fig. 7.

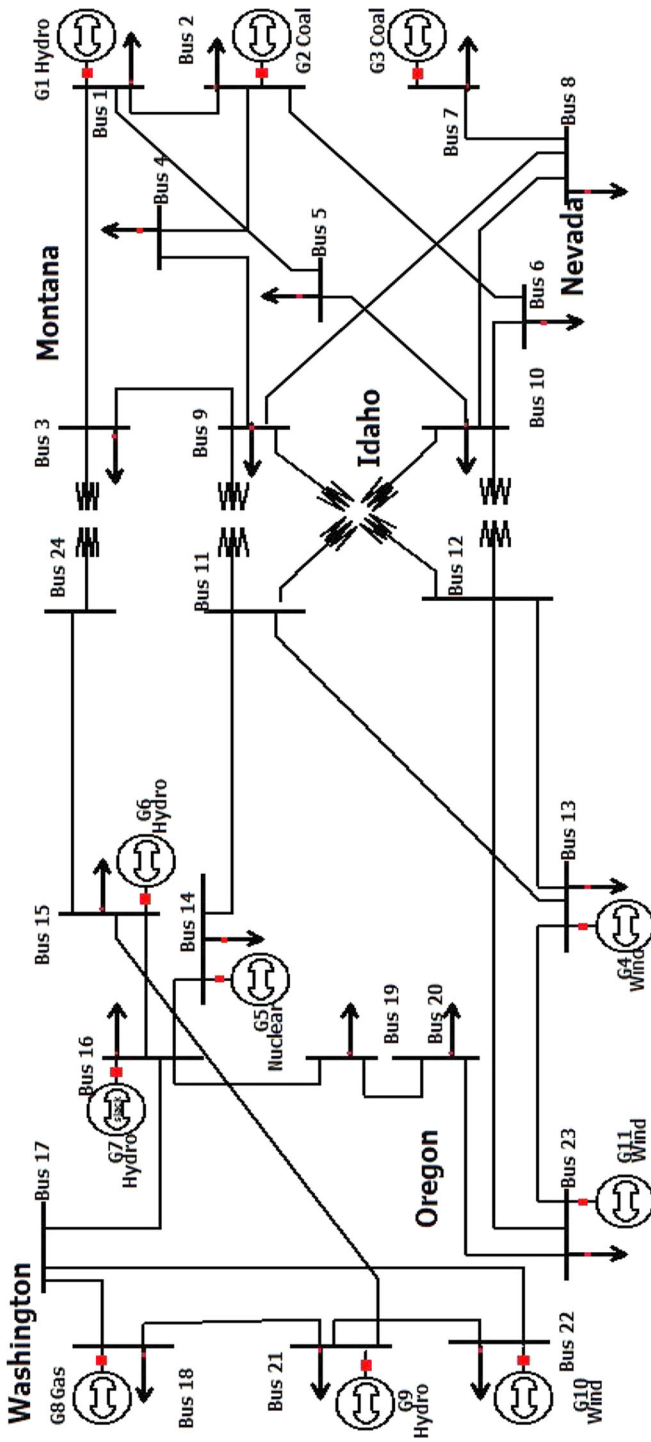


Fig. 7 A system network diagram with BPA's operation areas. This network has 24 electrical nodes and 11 power generators including hydro, coal, nuclear, natural gas and wind power. The installed generation capacity in the simulation system is configured according to the resources listed in Table 3

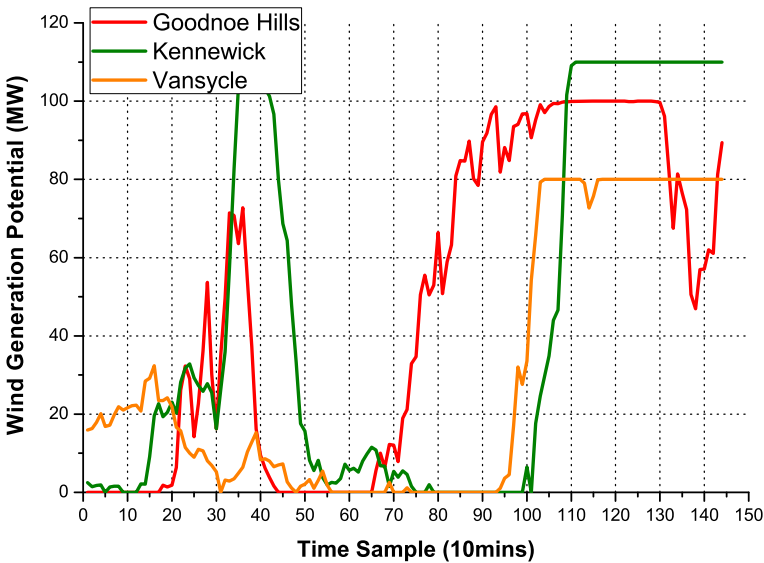


Fig. 8 The wind generation potential of Vansycle, Kennewick and Goodnoe Hills on 15 August 2003. The *horizontal axis* indicates different time steps with 10 min per interval, and the *vertical axis* indicates the wind production potential or available wind generation in MW

The load profile used in the simulation is scaled from the historical load profile of the BPA system (BPA 2007). Fourteen typical days in 7 months of different seasons are selected for simulation. The duration of a simulation is a typical power system operation period of 24 h ($T = 144$). The different wind forecast methods described in Sect. 2 are implemented in the simulation. The operating interval, ΔT , of generation scheduling is 10 min. Wind profiles during the selected 14 days are collected from the BPA system and scaled to the simulation system. For example, the wind generation potentials at the three locations ($n = 3$) on 15 August 2003 are presented in Fig. 8. Wind generation over the maximum generation capability of the wind turbines has to be curtailed for security purposes. The wind component for the reserve requirement is estimated by the MAE of the wind forecast errors. Because over-scheduling (the scheduled wind generation is higher than the actual production capability) requires deployment of additional reserve capacity, under-forecast errors are not considered in the MAE calculations. A coefficient of 1.2 is multiplied to the MAE value as a reliability margin.

Generator parameters are configured according to Gu and Xie (2010). In the simulation, the minimum output levels of conventional generators, $P_{G_i}^{\min}$, and wind generators, $P_{W_i}^{\min}$, are assumed to be zero. The total installed generation capacity is 4,000 MW. Of this total, the capacity of wind generation is 290 MW, which is about 7.3% (representative of a realistic BPA scenario). Table 4 lists the bus number (the number of the electrical node where the generator is located), type (what technology is used), capacity (Cap.: the total power capacity of the generator, in MW), marginal cost (M.C.: the marginal generation cost, which indicates the cost increment due to a power

Table 4 Each generator's configuration including capacity, marginal cost, and ramping rates

No.	Bus	Type	Cap. (MW)	M.C. (\$/MWh)	RP. (p.u.)
1	1	Hydro	400	6	0.08
2	2	Coal	200	37	0.0081
3	7	Coal	350	35	0.0085
4	13	Wind (GH)	100	3	0.1
5	14	Nuclear	110	21	0.004
6	15	Hydro	700	5	0.074
7	16	Hydro	650	3.7	0.059
8	18	Natural gas	500	79	0.051
9	21	Hydro	800	3.5	0.081
10	22	Wind (KW)	110	2	0.05
11	23	Wind (VS)	80	1	0.094

Table 5 Economic performance (in \$) of wind forecast methods for several days in 2003

Date▷	1-May	8-May	4-Jun	13-Jun	17-Jul	26-Jul	15-Aug
OB	813,729	783,258	824,637	678,908	832,347	729,972	724,894
PSS	891,771	895,812	887,321	874,657	884,629	920,145	892,553
AR	881,738	904,242	891,661	869,866	882,116	908,830	886,935
RRSTD	870,860	902,351	881,143	866,084	872,777	907,764	866,633
Date▷	28-Aug	1-Sep	15-Sep	3-Oct	31-Oct	17-Nov	20-Nov
OB	822,347	831,509	785,226	834,096	787,220	630,076	694,971
PSS	869,431	879,336	977,584	864,966	906,577	748,126	924,221
AR	878,986	883,951	961,685	863,474	905,447	733,469	914,903
RRSTD	865,374	872,161	961,574	864,207	913,095	751,672	901,549

The smallest cost is in bold

generation increase, in \$/MWh), and ramping rate (RP.: the capability of a generator to change its output per minute in normalized per unit value) of each generator.

4.4 Analysis of economic dispatch results

We present in Table 5 the performance of the economic dispatch model under different wind forecast models. The wind observation (OB), i.e., the true value, has the lowest system operating cost for all 14 days. Among different methods, the total operating costs from using PSS are relatively higher over the 14 days. The AR model, which considers only temporal wind correlations, results in a relatively modest cost-saving performance. The RRSTD model performs better than either PSS or AR models.

For most of the days, the RRSTD has a relatively higher cost savings than the other approaches. Among the 14 days, 15 August 2003 is selected for a detailed study as

Table 6 System operating results (in \$) on 15 August 2003

	OB	PSS	AR	RRSTD
Total Cost	724,894	892,553	886,935	866,633
Energy Market Cost	494,017	519,049	520,625	517,246
Regulation Cost	171,619	237,180	237,801	231,367
Reserve Cost	59,257	112,748	111,124	103,982
Deviation Penalty	0	23,576	17,385	14,038
Cost Reduced (%)	18.78	0.00	0.63	2.90

The smallest cost is in bold

Table 7 Wind location benefits analysis (in \$) on 15 August 2003

Location	Operating cost savings	Deviation penalty savings	Total cost savings
GH	956	3,289	4,245
KW	431	3,904	4,335
VS	1,197	2,345	3,542

reported in the remainder of this section. The operating results for this day are presented in Table 6. The row “Energy Market Cost” refers to the generation cost from all the generator units in the perspective of the system operator. The rows “Regulation Cost” and “Reserve Cost” give the total costs of providing regulation services and reserve services of all the units. The row “Cost Reduced” refers to the cost savings (in %) from using other forecasting models than the PSS model.

According to the simulation results, the RRSTD model increases the actual wind resource utilization, and reduces the system-wide generation cost, the system’s ancillary services (including regulation and reserve services) costs, the wind generation deviation penalty and the total system operating costs.

It can be observed in Table 6 that the system-wide operating cost using the RRSTD model is 2.90 % lower than that using the PSS model. One of the advantages of the RRSTD is the reduction in wind generation deviation. As shown in Table 6, the wind generation deviation penalty is reduced by almost 60 % when the RRSTD model is used compared with the PSS model and by 24 % compared with the AR model. The reduction in wind generation deviation is because space-time wind forecasts can increase the wind forecast accuracy (with lower MAE) and reduce the overestimation of available wind generation. In addition, the results of the RRSTD model reveal the advantage in the operating cost of ancillary services. For instance, the total costs of regulation and reserve services are reduced by 2.90 % when using the RRSTD model. Table 7 presents the economic benefits for each individual wind location. As we can see, using the RRSTD model, the operating cost can be reduced by up to 9 % and the generation deviation penalty can be reduced by up to 40 %. Given the same wind pressure and system load patterns, the space-time wind forecast model yields higher wind resources utilization and a higher wind generation ratio than the other models. This is because the increased accuracy of the space-time wind forecast model

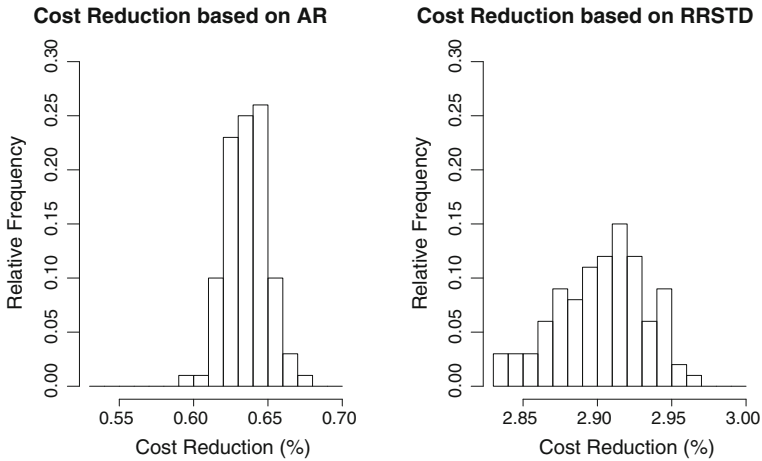


Fig. 9 Histograms of relative cost savings in percentage based on wind power forecasts from the AR and RRSTD models, compared with the costs based on forecasts from PSS

decreases the wind generation that would be wasted by underestimation of available wind generation potentials.

In addition, a simulation study is carried out to quantify the uncertainty on the 2.90 % cost saving on 15 August 2003. For every 10 min, 400 realizations are generated from the wind speed-predictive distribution for the AR and RRSTD models, respectively, and the median of the realizations is treated as the point forecast. This procedure is carried out 100 times. Hence, 100 wind speed forecasts are simulated for that day for every 10 min based on the AR and RRSTD models, respectively. Then the wind speed forecasts are converted to wind power with the 2.5 MW Nordex power curve and put into the power system dispatch model. Figure 9 displays the histograms of cost reductions of the system operations with the simulated wind power forecasts from AR and RRSTD, relative to the cost based on the forecasts from PSS. The 95 % confidence interval of relative cost savings for using forecasts from the AR instead of those from PSS is [0.61, 0.66 %] and it is [2.84, 2.95 %] for RRSTD. The concentrated histograms and narrow confidence intervals demonstrate that the variability of the cost reduction is small. Therefore, it is reliable to conclude that because of the improvement on the wind speed forecasting accuracy using the RRSTD model, the cost is reduced by around 2.90 % instead of using forecasts from PSS, while it is only 0.63 % with the AR model, on 15 August 2003. It should be noted that in this paper, we did not consider the impact of transmission congestion and contingency on the economic benefits analysis.

In Fig. 10 (top panel), the actual wind generation output at Kennewick is presented. The OB curve depicts the case when there is no wind forecast error, which gives the highest wind generation as well as the best economic dispatch performance. The wind generation profile using the PSS model has the lowest utilization of wind resources, while the wind generation profile of the AR model has the second lowest utilization result. By using the RRSTD model, more wind generation can be integrated into the power system. This is because the underestimation of available wind generation can

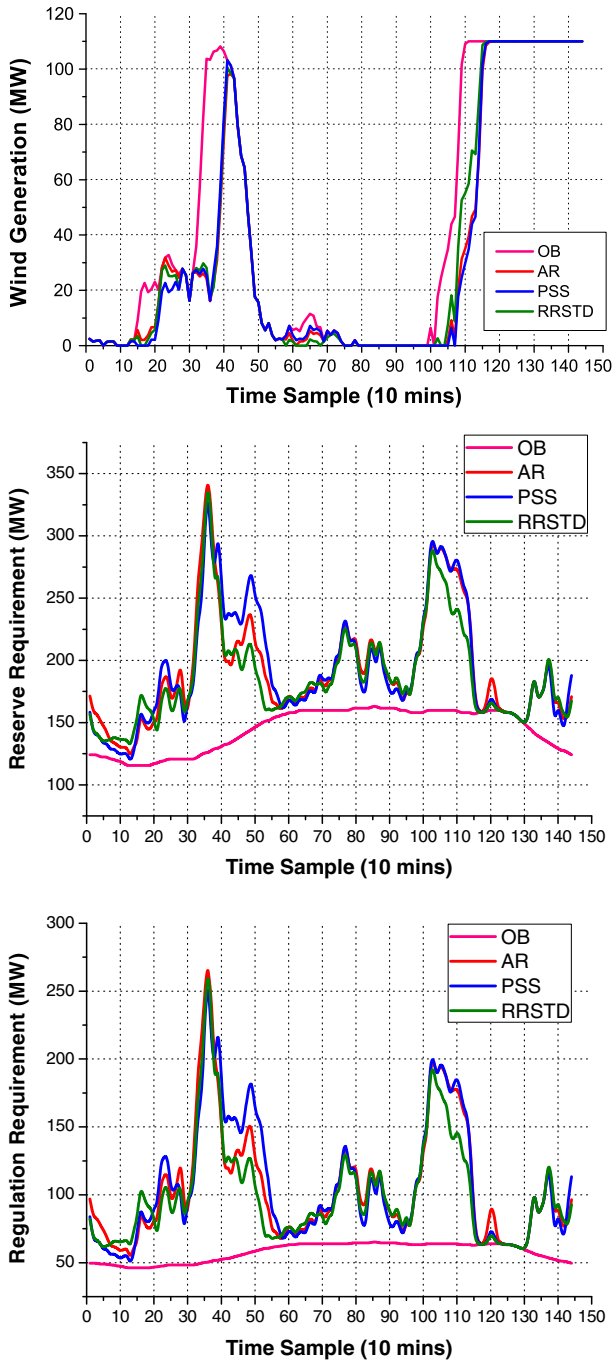


Fig. 10 Actual wind generation at Kennewick (*top panel*), total system reserve service requirement (*middle panel*), and total system regulation service requirement (*bottom panel*) on 15 August 2003, for different forecasting approaches including OB, PSS, AR, and RRSTD models

be avoided during the dispatch process because of the highly accurate wind forecasts by RRSTD and the potential for wind resources not being utilized is reduced.

The system's overall reserve requirement takes into account the uncertainty of both wind generation (mainly forecast errors) and load (demand forecast errors). The selected reserve capacity is used to compensate the energy imbalance within time frameworks of 30 min to 2 h. In Fig. 10 (middle panel), the total system reserve requirement for each model is compared. This panel shows that using the RRSTD model the overall reserve requirement can be reduced due to the improved forecast accuracy.

Regulating energy imbalances in the system keeps the system frequency within a secure range. Unlike reserve services, the capacity for regulation is used to smooth short-term (1–10 min) frequency fluctuations and energy imbalances. Figure 10 (bottom panel) shows that the RRSTD model decreases the requirement for regulation capacity, and therefore reduces the corresponding regulation cost.

Because of the reduction in both the total power generation cost and the ancillary services costs using the RRSTD model, the total operating cost is reduced by 2.90% compared with the results from the PSS model. Given that the market for electricity is significant (multi-billions of dollars in regions like Texas and about 240 million for BPA), a 2.90% savings in operating costs means tens of millions of dollars in cost savings due to improved wind forecasts.

5 Conclusion

Although wind power is increasingly important to the electricity supply market, the inclusion of wind power is a challenge to power system operations because of the high variations and limited predictability of wind. Advanced technologies that forecast wind accurately and loss functions that can evaluate forecasts more realistically are needed.

We introduced a new space-time model, the RRSTD model, to solve short-term wind speed forecasting problems. This model generalizes the RSTD model by allowing the forecast regimes to vary with the dominant wind direction and with the season without requiring much prior geographic information. Its forecasts are better than results from the PSS and AR models. We add that the RRSTD model has the potential to improve forecasts further if more information on monthly wind patterns are available.

Moreover, we proposed a new, realistic method to evaluate forecasts based on power system operating costs through a power system dispatch. To this end, we formulated an economic dispatch model that takes into account the space-time wind forecast information modeled by the RRSTD. Our space-time wind forecasting model reduces the cost of ancillary services, including regulation and reserve costs. These costs were reduced by 2.90% in a realistic illustrative example. Although the data set used in this study is fairly small and comes from a very specific microclimate, we believe that it illustrates the potential gains of combining accurate space-time wind forecasts that incorporate spatial correlation of wind patterns with electric power system scheduling. Similar conclusions have been obtained by Xie et al. (2014) with wind data from West Texas, whose geographical wind pattern is totally different from the Columbia River

Basin. As more wind data sets become available for research purposes, we welcome further studies and extensions of the methodologies developed in this paper.

In this paper, for the RRSTD model, we only considered the simplest case of two equally divided regimes based on the local wind patterns. More complex RRSTD models with more than two forecasting regimes or unequally divided regimes could be implemented in more complicated situations. Furthermore, there are other ways to perform the regime selection, such as using a Bayesian model selection framework, or an empirical analysis of out-of-sample data. In addition, an open challenge for further investigation is to develop an economic dispatch model that makes use of the full spatio-temporal predictive distribution that wind forecasting models can provide.

References

- Ackermann T (2005) Wind power in power systems. Wiley, New York. <http://books.google.com/books?id=NcMws2-N3BMC>
- Bouffard F, Galiana FD (2008) Stochastic security for operations planning with significant wind power generation. In: Proceeding of power and energy society general meeting—conversion and delivery of electrical energy in the 21st Century, 2008 IEEE, pp 1–11
- BPA (2007) BPA total transmission system load. Bonneville Power Administration
- BPA (2010) 2009 BPA facts. Bonneville Power Administration
- Constantinescu EM, Zavala VM, Rocklin M, Sangmin L, Anitescu M (2011) A computational framework for uncertainty quantification and stochastic optimization in unit commitment with wind power generation. *IEEE Trans Power Syst* 26(1):431–441
- CREIA (2010) CREIA 2010 China wind power outlook. China Renewable Energy Industries Association
- Denny E, O'Malley M (2006) Wind generation, power system operation, and emissions reduction. *IEEE Trans Power Syst* 21(1):341–347. doi:[10.1109/TPWRS.2005.857845](https://doi.org/10.1109/TPWRS.2005.857845)
- DOE (2008) 20 % Wind energy by 2030: increasing wind energy's contribution to U.S. electricity supply. The US Department of Energy
- Doherty R, O'Malley M (2005) A new approach to quantify reserve demand in systems with significant installed wind capacity. *IEEE Trans Power Syst* 20(2):587–595
- ERCOT (2010) ERCOT quick facts. Electric Reliability Council of Texas
- EWEA (2012) Wind in power: 2011 European statistics. The European Wind Energy Association.
- Genton MG, Hering AS (2007) Blowing in the wind. *Significance* 4:11–14
- Giebel G, Brownsword R, Kariniotakis G, Denhard M, Draxl C (2011) The state-of-the-art in short-term prediction of wind power: a literature overview, 2nd edn. ANEMOSplus
- Gneiting T (2011) Quantiles as optimal point forecasts. *Int J Forecast* 27:197–207
- Gneiting T, Raftery AE (2007) Strictly proper scoring rules, prediction, and estimation. *J Am Stat Assoc* 102:359–378
- Gneiting T, Larson K, Westrick K, Genton MG, Aldrich E (2006) Calibrated probabilistic forecasting at the stateline wind energy center: the regime-switching space-time method. *J Am Stat Assoc* 101:968–979
- Grigg C, Wong P, Albrecht P, Allan R, Bhavaraju M, Billinton R, Chen Q, Fong C, Haddad S, Kuruganty S, Li W, Mukerji R, Patton D, Rau N, Reppen D, Schneider A, Shahidehpour M, Singh C (1999) A report prepared by the reliability test system task force of the application of probability methods subcommittee. *IEEE Trans Power Syst* 14(3):1010–1020
- Gu Y, Xie L (2010) Look-ahead coordination of wind energy and electric vehicles: A market-based approach. In: Proceeding of North American power symposium 2010, The University of Texas, Arlington.
- Hering AS, Genton MG (2010) Powering up with space-time wind forecasting. *J Am Stat Assoc* 105:92–104
- Jeon J, Taylor JW (2012) Using conditional kernel density estimation for wind power density forecasting. *J Am Stat Assoc* 107(497):66–79. doi:[10.1080/01621459.2011.643745](https://doi.org/10.1080/01621459.2011.643745)
- Kariniotakis G, Pinson P, Siebert N, Giebel G, Barthelmie R (2004) The-state-of-the-art in short-term prediction of wind power - from an offshore perspective. In: Proceeding of symposium ADEME, IFREMER.
- Makarov Y, Lu S, McManus B, Pease J (2008) The future impact of wind on bpa power system ancillary services. In: Proceeding of transmission and distribution conference and exposition, IEEE/PES.

- Makarov Y, Loutan C, Ma J, de Mello P (2009) Operational impacts of wind generation on california power systems. *IEEE Trans Power Syst* 24(2):1039–1050. doi:[10.1109/TPWRS.2009.2016364](https://doi.org/10.1109/TPWRS.2009.2016364)
- Meibom P, Barth R, Hasche B, Brand H, Weber C, O'Malley M (2011) Stochastic optimization model to study the operational impacts of high wind penetrations in ireland. *IEEE Trans Power Syst* 26(3):1367–1379
- Monteiro C, Keko H, Bessa R, Miranda V, Botterud A, Wang J, Conzelmann G (2009) A quick guide to wind power forecasting: stat-of-the-art 2009.
- Papavasiliou A, Oren SS, O'Neill RP (2011) Reserve requirements for wind power integration: a scenario-based stochastic programming framework. *IEEE Trans Power Syst* 26(4):2197–2206
- Pappala VS, Erlich I, Rohrig K, Dobschinski J (2009) A stochastic model for the optimal operation of a wind-thermal power system. *IEEE Trans Power Syst* 24(2):940–950
- Pinson P, Madsen H (2012) Adaptive modeling and forecasting of wind power fluctuations with markov-switching autoregressive models. *Int J Forecast* 31:281–313
- Soder L (2004) Simulation of wind speed forecast errors for operation planning of multiarea power systems. In: *Proceeding of probabilistic methods applied to power systems, 2004 international conference on*, pp 723–728
- Tastu J, Pinson P, Kotwa E, Nielsen H, Madsen H (2011) Spatio-temporal analysis and modeling of wind power forecast errors. *Int Stat Rev* 14:43–60
- Tuohy A, Meibom P, Denny E, O'Malley M (2009) Unit commitment for systems with significant wind penetration. *IEEE Trans Power Syst* 24(2):592–601
- Wang J, Shahidehpour M, Li Z (2008) Security-constrained unit commitment with volatile wind power generation. *IEEE Trans Power Syst* 23(3):1319–1327
- Watson SJ, Landberg L, Halliday JA (1994) Application of wind speed forecasting to the integration of wind energy into a large scale power system. *Gener Transm Distrib IEEE Proc* 141(4):357–362
- Wu L, Shahidehpour M, Li T (2007) Stochastic security-constrained unit commitment. *IEEE Trans Power Syst* 22(2):800–811
- Xie L, Carvalho P, Ferreira L, Liu J, Krogh B, Popli N, Ilić M (2011) Wind energy integration in power systems: operational challenges and possible solutions. In: *Special issue of the proceedings of IEEE on network systems engineering for meeting the energy and environment dream* 99(1):214–232
- Xie L, Gu Y, Zhu X, Genton MG (2014) Short-term spatio-temporal wind power forecast in robust look-ahead power system dispatch. *IEEE Trans Smart Grid* 5:511–520
- Zhao L, Zeng B (2010) Robust unit commitment problem with demand response and wind energy. University of South Florida, Technical Report, USA
- Zhu X, Genton MG (2012) Short-term wind speed forecasting for power system operation. *Int Stat Rev* 80:2–23